Numerical Analysis of In-Situ Methane Hydrate Formation in Sandstone

HUSEBØ, J., KVAMME, B., GRAUE, A.
Department of Physics and Technology
University of Bergen
Allégaten 55, 5007 Bergen
NORWAY
http://web.ift.uib.no/php/php/agraue.html

Abstract: - The energy related to natural gas trapped in water as hydrate may be twice the amount of all known sources of conventional oil, gas and coal. Fundamental understanding of the dynamics of the phase transitions for hydrate formation and dissociation is crucial in the design of efficient exploitation strategies for these types of hydrocarbon resources. Magnetic Resonance Imaging (MRI) is a powerful tool for imaging these phase transitions. A single MRI image consists of an enormous amount of raw, unprocessed data. In this work we describe an in-house built software that has proven to be highly efficient in storing, structuring and analyzing these data. The program also removes background noise and assists in identifying anomalies, making it possible to do real time in-situ analysis of complex hydrate experiments in both bulk and porous media. We demonstrate application of this program through a specific experiment of hydrate formation in Bentheimer sandstone.

Key Words: - Methane hydrate, MRI, IDL-programming, software development

1 Introduction

Methane hydrate is a clathrate compound where methane molecules are trapped inside cavities of hydrogen bounded water molecules. Macroscopically hydrate appears similar to ice and snow. However, unlike ice hydrate is stable above zero Celsius if the pressure is sufficiently high.

Worldwide there are huge amounts of natural gas trapped in the form of hydrate. The estimated energy potential is twice that of the combined contribution from conventional oil, gas and coal [1, 2]. Internationally there is an increasing interest in commercial exploitation of hydrate, as seen by substantial national research programs like for instance the Japanese program MH21 [3]. Relative to the stability regions of natural gas hydrate there is essentially two different ways to release the natural gas from the hydrate. A first set of approaches changes the thermodynamic conditions so as to bring the hydrate out from the stability region. Typical strategies are pressure reduction, addition of heat or addition of chemicals which alters the chemical potential of liquid water. Carbon dioxide hydrate is thermodynamically more stable than natural gas hydrate [4 – 6]. Exploitation of natural gas hydrate reservoirs through injection of carbon dioxide is a win-win situation which also may provide long term safe storage of carbon dioxide [7, 8].

Fundamental understanding of the dynamics related to hydrate formation and dissociation is crucial for the design of efficient exploitation schemes. Some elements of the dynamic features might be explored in the absence of realistic reservoir structures but the impact of interactions between minerals [9] on the stability of surrounding phases makes it necessary to conduct experiments in realistic porous media.

In this work methane hydrate is formed in sandstone cores to create experimental representation of natural gas hydrate reservoirs. The hydrate formation rate and pattern is monitored in-situ by using Magnetic Resonance Imaging (MRI). MRI can be used because the nuclear magnetic relaxation time of hydrogen decreases significantly as the system goes from a gas-water state to a gas-solid state.

A single MRI image consists of an enormous amount of raw, unprocessed data. Generating and analyzing a series of consecutive MRI scans makes it apparent that a software based analysis tool is needed in order to store, structure and optimize these data. In this work we describe an in-house built software called ROI (Region Of Interest) [10]. The program has a Graphical User Interface (GUI) and is developed using Interactive Data Language (IDL) [11]. ROI can monitor the rate and pattern of both the hydrate formation and dissociation. It can also help to identify anomalies such as RF-artifacts,

localized hydrate dissociation and position dependent changes in background noise. The ROI-program makes it possible to do real time in-situ analysis of complex hydrate experiments in both bulk and porous media.

The paper is organized as follows. The experimental approach is described in section 2 followed by relevant examples related to methane hydrate formation (section 3). Discussion in section 4 followed by our conclusions in section 5.

2 Experimental approach

2.1 Experimental setup

The experimental design included a pressure- and temperature-controlled sample holder with several ports for fluid flow placed inside the bore of a Magnetic Resonance Imager (see Fig. 1). The core holder was constructed with special wound s-glass fiber, embedded in a catalyzed resin for strength, that has a low inductance to minimize distortion of the MRI images compared to cells made from conventional glass fiber. The sample holder has a series of ports for gas and liquid supply to the core along with ports associated with a pressurized core-holder sleeve. Fluorinert (FC-84) was used as a combination pressure control and cooling fluid for the sample holder; since it lacks hydrogen it is not detected by the MRI. The efficiency of the fluid-cooling system was such that the sample holder was cooled from 25^{o}C to 4^{o}C in 3 hours and remained stable within 0.1^{o}C for the duration of an experiment that lasted up to several months. The sample was encased in shrink-wrap Teflon acting as a sleeve protecting the core from the Fluorinert and preventing the flow directed through the core to bypass along the edges. A confining pressure of 10.2 MPa was placed on the sample. Gases and liquids were introduced to the sample at 8.2MPa pore pressure. Fluid volumes, pressures and temperatures were monitored at inlet and outlet ports on the sample holder through a series of data acquisition stations.

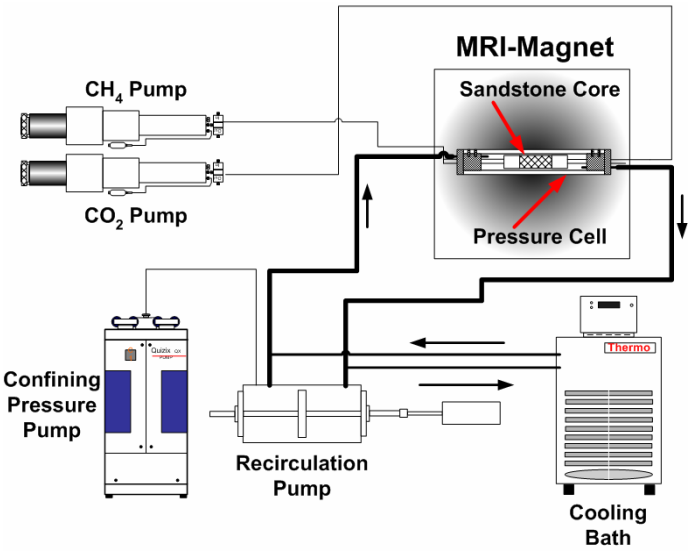

Fig. 1, Schematic diagram of experimental setup

2.2 Sampling and data analysis

MRI data were collected at intervals during the hydrate formation to provide spatial information on the distribution of hydrogen-bearing fluids in the pores and larger open volumes. The MRI intensity was used along with temperature and volume data to monitor changes in-situ. Measurements were made in a small-bore, 310mm, 2.0T superconducting magnet that comfortably holds the core holder and external insulation that was used to control humidity around the cell. The hydrogen resonance frequency of 87.71 MHz, along with offsets and pulse-width parameters were checked on a regular basis. Standard Hahn spin-echo pulse sequences were used to acquire 1-D profiles, 2-D and 3-D images. The varying information requirements during the experiment dictated the type of data acquisition performed. Fast 1-D profiles were used to monitor the establishment of initial saturations in the sample while 2-D and 3-D images were designed for collecting higher signal-to-noise image data needed for quantitative analysis of fluid abundances and spatial distributions.

The acquisition of suitable quality images was challenging given the range of relaxation times associated with the fluids in this experimental system. The T1 and T2 relaxation time for bulk CH_4 and water is in the 1 to 2 second range while the water in partially saturated pores has T1 of 0.8 – 1.5 second and T2* of 50-100 milliseconds depending upon the actual water saturation. This range of T1 relaxation time required relatively long recovery times between spin echo pulse sequences, generally 4 to 8 seconds, to ensure significant polarization of the bulk fluids, but short echo times to

collect significant signal. The trade-off was between running a sufficiently long recovery time and keeping the total image acquisition time as short as possible to increase the time resolution. In some images complete polarization of the slowest relaxing fluids was sacrificed for shorter recovery times and reasonable acquisition times. High quality 3-D images of 128 x 32 x 32 voxels arranged over the length of the sample holder, 120mm x 60mm x 60mm, required 9 hours for acquisition. This provided a spatial resolution of 0.94 x 1.88 x 1.88 mm. The minimum echo spacing for the spin-echo acquisition permitted with this instrument is 3 to 2.2 milliseconds, which is relatively slow when attempting to measure relaxation processes in porous media. It is likely that some signal intensity was lost due to diffusion processes that occur during the long inter-echo time and the use of short recovery times.

3 Hydrate Formation and analysis

Hydrates were formed in a water and methane saturated porous sandstone, with 52% water saturation, at a temperature of 4°C and a pressure of 8.2MPa. The Bentheim sandstone exhibits quite pure mineralogy, 99% quartz, a porosity of 22%, and a fairly high permeability, 1.1 Darcy [12]. Average pore size was 120 microns as determined by optical microscopy. The absence of paramagnetic minerals in this sandstone made it suitable for MRI imaging experiments.

3.1 Forming of hydrates in sandstone core

The sandstone samples used in these experiments consisted of halves of cylindrical plugs separated by a spacer that simulated a longitudinal fracture or fluid conduit in the sample (see Fig. 2). The 4mm thick spacer made of high molecular-weight polyethylene consisted of a frame the length of the core sample with two large void spaces that were connected by narrow half-circle openings in the frame that permitted easy access of fluids to the open region. The core halves and spacer were machined such that when assembled they formed a 3.8 cm diameter cylinder that fitted snugly within the pressurized sleeve of the core holder. These fractured core experiments focused on monitoring rates of hydrate formation and exchange that were accelerated by the fluid pathway down the length of the core.

Fig. 2; Picture of fractured core and spacer

The steps to establish initial water and gas saturations in the pores of the sandstone core were critical for the rapid formation of hydrates in the laboratory. The procedure began with evacuating the dried core. Then the system was pressurized to 8.2MPa using methane. Sufficient water was then injected into the spacer region to fill the desired fraction of the pore volume. The water-wet nature of the sandstone resulted in rapid imbibition of the water from the spacer into the pores. The challenge was to establish a uniform distribution of water throughout the length of the core as determined by rapid 1-D and 2-D MRI images of the water-saturated core. Water was injected stepwise to even the distribution of water throughout the length of the core. MRI images collected at this point are characterized by relatively high signal-to-noise levels as much of the intensity derives from the free water in the pores, along with free methane in the pore space and the spacer interval between the core halves.

After the initial water and methane saturations were established in the core and measured the core holder was cooled from 25^{o} to 4^{o}C over a several hour period. During this short interval MRI intensity increase coincided with an increase in methane consumption as monitored by the external pump. This increase with temperature decrease corresponded to the density change associated with the cooling of the methane and was within 5% of anticipated volume changes based on known pore volumes and standard gas calculations [13]. This increase is also evident in the methane log seen in Fig. 3-A.

Once the sample reached 4^{o}C there was a 1 hour period of no measurable change in the MRI intensity and

the methane pump volume. After this induction period there was a rapid decrease in overall MRI intensity measured in the core and a concomitant increase in methane pump volume as additional methane was added to the hydrate-water-gas system (see Fig. 3 and Fig. 4). The decrease in MRI intensity asymptotically approached a non-zero value that represents the contribution of residual water not transformed into hydrate and free methane in the open pore space. The hydrate formation experiment had some residual water remaining in the pores, generally less than 20% of the original amount. The 3-D MRI images provided clear evidence that this residual water was localized in small regions rather than distributed uniformly throughout the core (see Fig. 4-D).

3.2 Analysis of hydrate formation using ROI

ROI can perform real time in-situ analysis during the experimental progress by monitoring the MRI-signal distribution, within a defined region of interest, as a function of both time and space. This information is helpful when determining the hydrate formation rate (see Fig. 3), and crucial when determining the distribution of injected water (see Fig. 5) as well as the hydrate formation pattern (see Fig. 6).

Electromagnetic background noise may interfere with the magnetic field or the electronics of the MRI. This interference reduces the signal-to-noise ratio and impacts the ability to monitor the experimental progress (see Fig. 7). The ROI program has an algorithm capable of taking both directional and non-directional interference into account. The validity of the numerical analysis is much more robust, when applying the noise reduction algorithm found in the ROI program. The algorithm has been tested in numerous hydrate experiments, and has proven to give highly reproducible results.

4 Discussion

No consistent single hydrate growth pattern is found in this study. In some experiments the hydrate formed at one end of the core sample and progressed in a piston-like fashion towards the other end [7, 8]. This hydrate formation behavior was contrasted by other experiments where hydrate formation was distributed fairly uniformly throughout the core (see Fig. 6). Although there was no single pattern of hydrate growth observed at the resolution of these experiments that provided insights to nucleation and growth models, in most experiments almost all of the water was turned into hydrate.

Some portions of the observed variations between individual experiments can be assigned to natural variations in the gas (methane) and liquid (water) filling characteristics and corresponding gas pockets, local droplets and inhomogeneous wetting of the core.

5 Conclusions

We have presented a new numerical tool for analyzing the large amount of data obtained from Magnetic Resonance Imaging experiments of methane hydrate formation in sandstone. The use of this program significantly improved the analysis of the hydrate experiments, both with respect to speed, improved visualization and accuracy of the numerical analysis.

Using this tool we observed different formation patterns from different experimental runs, which was partly due to randomness incurred by gas and liquid dynamics during filling of the core. Corresponding distribution of gas pockets, liquid droplets and inhomogeneous filling of the pores were likely to play a significant role in variation from one experiment to the next. With ROI it was possible to perform real time in-situ analysis of hydrate experiments as well as identifying different large and small scale occurrences in the MRI data.

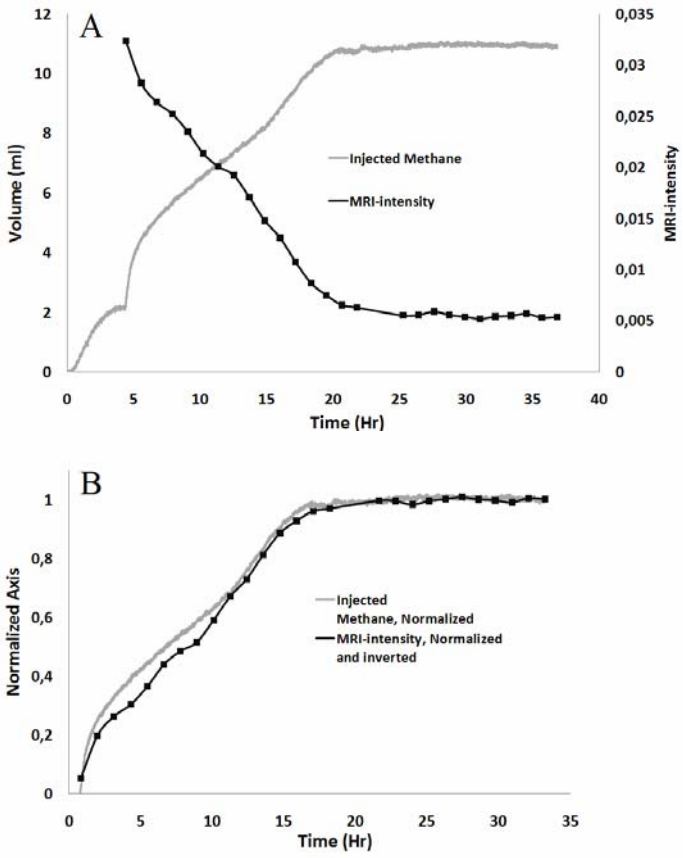

Fig. 3, A: Methane injected and reduction in MRI-intensity during hydrate formation. The initial injection of methane is due to the temperature reduction. B: Correlation between injected methane and MRI-intensity during methane hydrate formation. The MRI-intensity plots are generated using the ROI software.

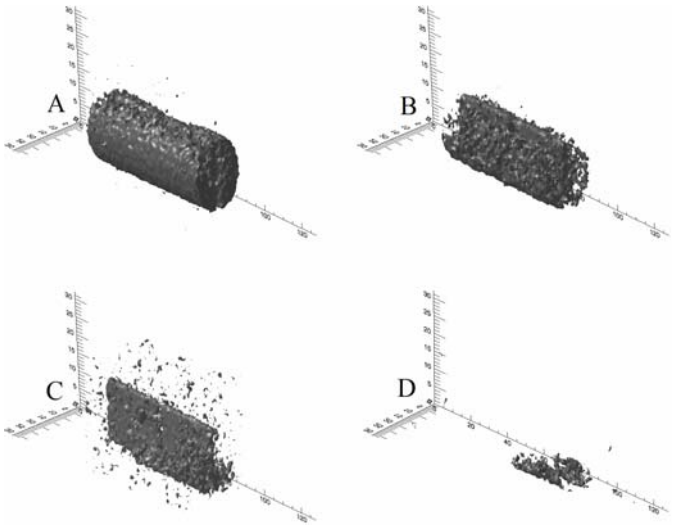

Fig. 4, A: Before cooling. B: hydrate has formed for 10hours. C: Hydrates has stopped forming, the fracture is filled with methane. There is a poor signal-to-noise ratio. D: Methane has been flushed out of the fracture, only residual water is visible. A,B and C are 1-hour scans, while D is a 9-hour scan.

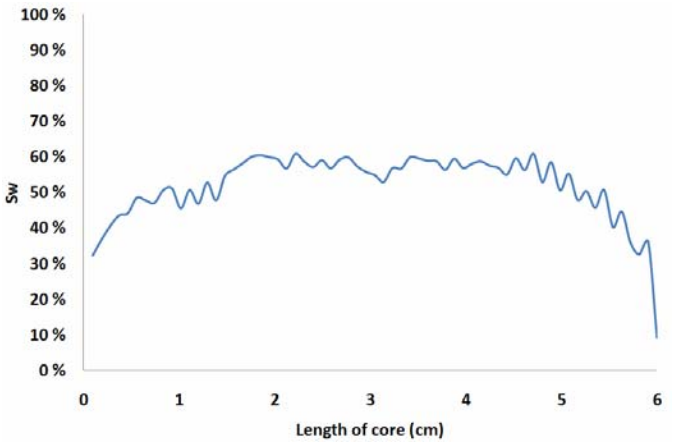

Fig. 5. Water distribution throughout the core, generated from a 9-hour scan.

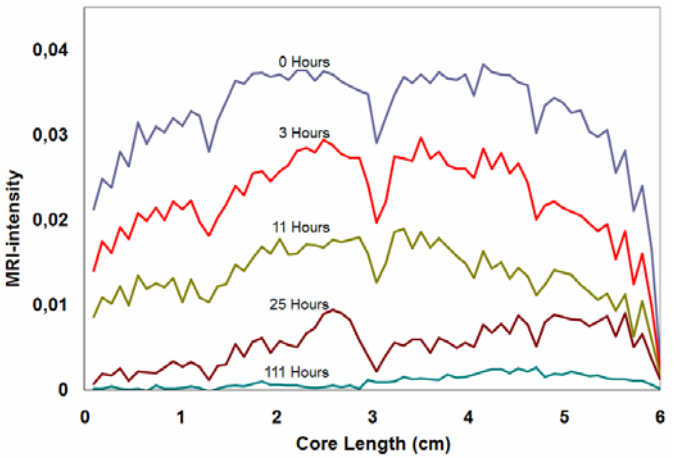

Fig. 6. Hydrate formation pattern. Hydrates are formed at equal rate throughout the core. Graphs are generated from consecutive 1 hour scans.

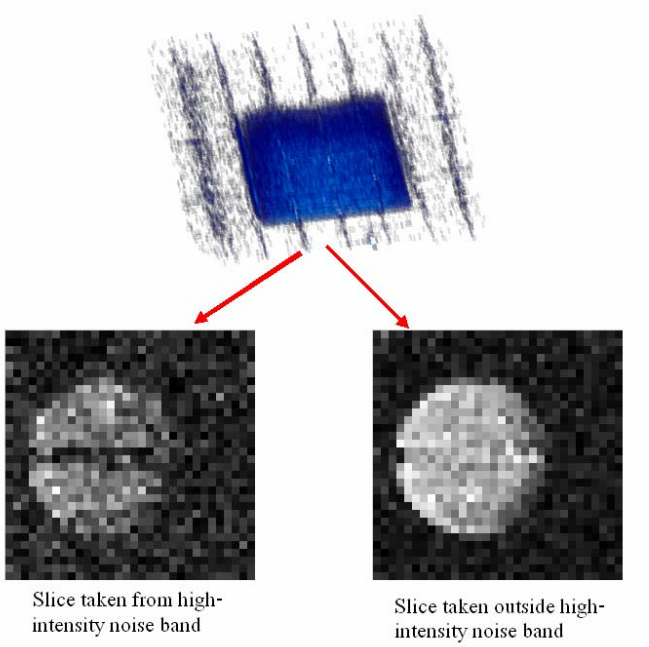

Fig. 7, MRI image with recurrent high intensity noise bands in the transverse direction. The slices taken out illustrates how the high intensity noise reduces signal-to-noise ratio. Screenshots from the ROI-software

References:

[1] L. Milich, Global Environmental Change – Human and Policy Dimensions, 1999, **9**, 179

[2] K. A. Kwenvolden, Proc. Natl. Acad. Sci. USA, **96**, 1999, 3420

[3] http://www.mh21japan.gr.jp/english/index.html

[4] Svandal, A., Kuznetsova, T., Kvamme, B., " *Thermodynamic properties interfacial structures and phase transitions in the $H_2O/CO_2/CH_4$ system*", Fluid Phase Equilibria, 2006, 246, 177–184

[5] Svandal, A., Kuznetsova, T., Kvamme, B., " *Thermodynamic properties and phase transitions in the $H_2O/CO_2/CH_4$ system*", Physical Chemistry Chemical Physics, 2006, **8**, 1707 - 1713

[6] Kvamme, B., Tanaka, H.: "*Thermodynamic stability of hydrates for ethylene, ethane and carbon dioxide*". J.Phys.Chem., 99, 7114, 1995

[7] Graue, A., Kvamme, B., Baldwin, B.A., Stevens, J., Howard, J., Ersland, G., Husebø, J., Zornes, D.R., *"Magnetic Resonance Imaging og Methane – Carbon Dioxide Hydrate Reactions in Sandstone Pores*", SPE 102915, 2006

[8] Graue, A., Kvamme, B., Baldwin, B.A., Stevens, J., Howard, J., Aspenes, E., Ersland, G., Husebø, J., Zornes, D.R., *"Environmentally Friendly CO2 Storage in Hydrate Reservoirs Benefits from Associated Spontaneous Methane Production*", SPE, OTC 18087, 2006

[9] Kvamme, B, Graue, A., Kuznetsova, T., Buanes, T., Ersland, G., "S*torage of CO2 in natural gas hydrate reservoirs and the effect of hydrate as an extra sealing in cold aquifers*", 2006, International Journal of Greenhouse Gas Control, in press

[10] Husebø, J., "*Instructions for ROI v2.0; A Comprehensive Outline of the ROI v2.0 Functionalities*", Internal document, University of Bergen/ConocoPhillips, 2006

[11] IDL 6.3, ITT Visual Information Solutions, http://www.ittvis.com/idl/, 2005

[12] Kvamme, B, Graue, A.,Aspenes, E., Kuznetsova, T., Gránásy, L., Tóth, G., Pusztai, T.,Tegze G., *"Towards understanding the kinetics of hydrate formation: Phase field theory of hydrate nucleation and magnetic resonance imaging"*, Physical Chemistry Chemical Physics, 2004, **6**, 2327 – 2334

[13] REFPROP, NIST Standard Reference Database 23, Version 7.0, National Institute of Standards and Technology, 2006